Available online at www.sciencedirect.com
SCIENCE DIRECT
Chemical Physics Letters 422 (2006) 354–357
CHEMICAL PHYSICS LETTERS
www.elsevier.com/locate/cplett

The role of charge-transfer integral in determining and engineering the carrier mobilities of 9,10-di(2-naphthyl)anthracene compounds

S.C. Tse [a], S.K. So [a,*], M.Y. Yeung [b], C.F. Lo [b], S.W. Wen [c], C.H. Chen [c]

[a] *Department of Physics and Centre for Advanced Luminescence Materials, Hong Kong Baptist University, Kowloon Tong, Hong Kong, China*
[b] *Department of Physics, The Chinese University of Hong Kong, Shatin, N.T., Hong Kong, China*
[c] *Department of Applied Chemistry, Microelectronics & Information Systems Research Center, National Chiao Tung University, Hsinchu, Taiwan, ROC*

Received 2 February 2006; in final form 20 February 2006
Available online 28 February 2006

Abstract

The charge transporting properties of *t*-butylated 9,10-di(2-naphthyl)anthracene (ADN) compounds have been investigated experimentally and computationally in relation to their molecular structures. The ADN compounds are found to be ambipolar with both electron and hole mobilities in the range of $1–4 \times 10^{-7}$ cm^2 V^{-1} s^{-1} (electric field 0.5–0.8 MV/cm). As the degree of *t*-butylation increases, the carrier mobility decreases progressively. The mobility reduction was examined by Marcus theory of reorganization energies. All ADN compounds possess similar reorganization energies of ~0.3 eV. The reduction of carrier mobilities with increasing *t*-butylation can be attributed to a decrease in the charge-transfer integral or the wavefunction overlap.

1. Introduction

There are increasing interests in studying the relationship between the charge transporting properties of organic electronic materials and their molecular structures [1]. Technologically, organic electronic materials are widely used in emerging electronic devices including organic light-emitting diodes (OLEDs) [2,3], solar cells [4], and thin film transistors [5,6]. Thus, there is a clear need to control and improve their solid state charge transporting properties for achieving device optimization. Fundamentally, the mechanisms of charge transport in organic electronic materials are still not well understood. This is especially true for amorphous organic electronic materials that have molecules with weak intermolecular interactions. There are two approaches to describe the charge transport in amorphous organic materials. The first approach deals with charge transport macroscopically. The organic electronic material is treated as an ensemble of disordered hopping sites through which injected carriers drift under the influence of an external applied field. The charge hopping rate is controlled by the energetic and the geometric disorders of the materials [7,8]. The second approach deals with the transport process microscopically. The rate limiting step is the intermolecular hopping between two adjacent molecules. In the absence of external forces, the rate, k, of electron or hole hopping can be described by the Marcus theory [9]:

$$k = \frac{4\pi^2}{h} \cdot V_{ab}^2 \cdot \frac{\exp(-\lambda/4k_B T)}{\sqrt{4\pi\lambda k_B T}}. \quad (1)$$

In Eq. (1), V_{ab} is the charge-transfer integral, λ is the reorganization energy, k_B is the Boltzmann's constant, T is the absolute temperature, and h is the Planck's constant. For a fixed T, the charge hopping rate k depends critically on two material parameters, namely, V_{ab} and λ. The reorganization energy is an intramolecular property that can be computed directly from techniques of quantum chemistry. On the other hand, the charge-transfer integral V_{ab} is the electronic coupling factor. It cannot be evaluated from first principle for amorphous materials because it depends precisely on how the frontier orbitals overlap in the solid state. Despite the challenges of finding V_{ab}, the latter approach is

* Corresponding author. Fax: +86 852 3411 5813.
E-mail address: skso@hkbu.edu.hk (S.K. So).

0009-2614/$ - see front matter © 2006 Elsevier B.V. All rights reserved.
doi:10.1016/j.cplett.2006.02.079

quite appealing as it provides a framework that can correlate microscopic molecular design to macroscopic carrier mobilities. So there are increasing theoretical or computational endeavors in research along this direction [10–12]. However, experimental investigations are lacking in clarifying the roles of λ and V_{ab} in carrier transport properties in amorphous organic materials.

This Letter experimentally and computationally addresses the interplay between V_{ab} and λ in affecting the carrier mobilities of a family of *tertiary*-butyl (*t*-Bu) substituted anthracene derivatives (ADN). The chemical structure of ADN is shown in Fig. 1. Experimentally, we observed that there is a systematic reduction in carrier mobilities in ADN as the number of *t*-Bu groups increases. By correlating the experimental observations with computational results, it can be shown that mobility reduction in ADN compounds is mainly controlled by V_{ab}, rather than λ.

2. Experimental

The ADN compounds are: (1) ADN – 9,10-di(2-naphthyl) anthracene, (2) TBADN – 2-*t*-butyl-9,10-di(2-naphthyl) anthracene, (3) DTBADN – 2,6-di(*t*-butyl)-9,10-di(2-naphthyl) anthracene, and (4) TTBADN – 2,6-di(*t*-butyl)-9,10-di-[6-(*t*-butyl)(2-naphthyl)]anthracene. All ADN compounds were synthesized according to a procedure outlined in the literature [13] and were purified by train-zone sublimation. ADN is now a well-recognized blue host material for OLED applications [14,15]. Therefore, it is important to measure their charge transporting properties. The carrier mobilities of ADN compounds were measured by optical time-of-flight (TOF) technique. Details of the time-of-flight (TOF) experimental setup were described elsewhere [16]. Briefly, the samples were prepared by thermal evaporation on indium-tin-oxide (ITO) substrates. The general sample structure is ITO/ADN compound (d μm)/Al (15 nm), where d varied between 5 and 7 μm. Films of ADN prepared this way were all found to be amorphous as indicated by the absence of any discernible X-ray diffraction peaks. After coating, the sample was immediately housed inside a vacuum cryostat for TOF measurements. A DC power supply was used to provide the necessary bias voltage to the sample for the relevant carrier detection. A N_2 laser at 337.1 nm was used to generate a sheet of free charges near one side of the sample. The injected carriers moved through the sample under the external electric field and drifted to the counter electrode. A current sensing resistor R in series with the sample converted and magnified the photocurrent to voltage readings. The value of R was adjusted between 1 and 1 MΩ so that the RC time constant should be at least 20 times less than the carrier transient time. A digital oscilloscope was used to capture the voltage across R.

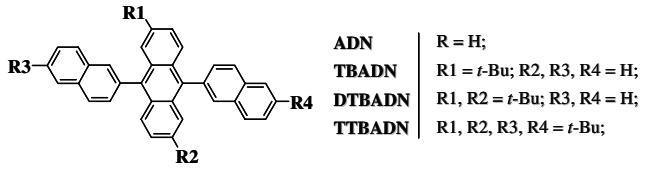

Fig. 1. Chemical structure of anthracene derivatives.

3. Results

Fig. 2 shows typical hole TOF time transient signals at 290 K under an electric field strength F. The photocurrent transients for all materials generally exhibit non-dispersive behaviors as characterized by a plateau and a well-defined turning point at time $t = \tau$, which is the flight time of carriers (inset). Fig. 3 shows the field dependent mobilities of all ADN compounds. The mobilities are obtained by the well-known relation $\mu = d^2/(V_{dc} \cdot \tau)$, where V_{dc} is the applied voltage. From Fig. 3, all the mobilities of ADN compounds at 290 K follow the Poole–Frenkel (PF) form, $\mu = \mu_0 \exp(\beta\sqrt{F})$, where β is the PF slope, and μ_0 is the zero-field mobility. Generally, both the ADN hole and electron mobilities are in the range $1–4 \times 10^{-7}$ cm^2 V^{-1} s^{-1} for F between 0.5 and 0.8 MV/cm at room temperature. Moreover, for a given ADN compound, the hole and electron mobilities are almost the same, indicating that ADN compounds are ambipolar. Furthermore, a systematic reduction in both the hole and the electron mobilities can be observed as the number of *t*-Bu groups increase. This Letter primarily addresses the last observation.

In the absence of any field ($F = 0$), the zero-field hole mobility, ($\mu_{h,0}$), only depends on λ – the reorganization

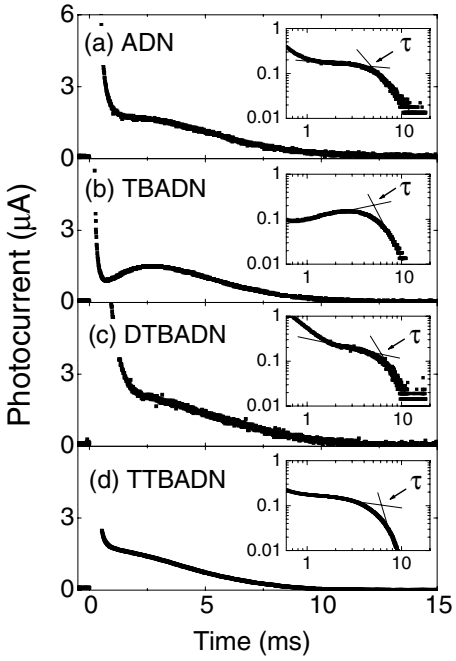

Fig. 2. TOF hole photocurrent plots at 290 K under applied field strength F for (a) ADN, $F = 0.56$ MV/cm; (b) TBADN, $F = 0.8$ MV/cm; (c) DTBADN, $F = 1.14$ MV/cm and (d) TTBADN, $F = 1.45$ MV/cm. The film thickness were 6.11 μm, 5.52 μm, 5.61 μm and 5.50 μm, respectively. The insets are log–log plots of the TOF transients.

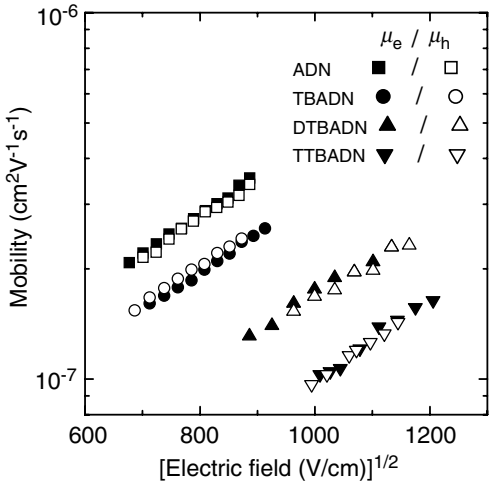

Fig. 3. Field dependent electron and hole mobilities of ADN, TBADN, DTBADN and TTBADN at 290 K.

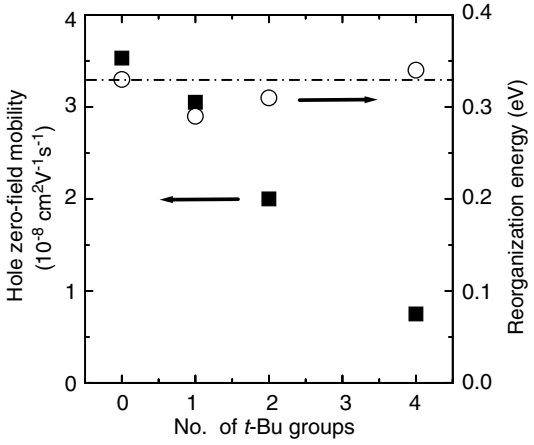

Fig. 4. Solid squares: experimentally extrapolated zero-field mobilities; Open circles: computationally determined reorganization energies against the number of *t*-Bu groups on ADN compounds at room temperature. The dashed line is the reorganization energy of the un-substituted ADN.

energy, and V_{ab} – the charge-transfer integral, as suggested by Eq. (1). Using Fig. 3, one can extract $\mu_{h,0}$ by linear extrapolation the hole mobilities to $F = 0$. The zero-field hole mobilities, which are measures of λ and V_{ab}, were summarized in Table 1 (second column) and in Fig. 4. (From this point onwards, we will confine our discussion in hole transport in ADN, but analogous arguments can be used to discuss electron transport.) Clearly, the TOF results suggest that increasing *t*-Bu substitution decreases the hole mobility.

4. Discussions

In order to understand the origin of mobility reduction in ADN after *t*-Bu substitution, we normalized the experimentally determined $\mu_{h,0}$ to that of the un-substituted ADN. The results are shown in Table 1 (third column). The values are 0.86, 0.57, and 0.21, for TBADN, DTBADN, TTBADN, respectively. According to Eq. (1), the normalized zero-field mobilities, can be written as

$$\frac{k}{k_{ADN}} \approx \left(\frac{V_{ab}}{V_{ADN}}\right)^2 \cdot \left[\left(\frac{\lambda_{ADN}}{\lambda}\right)^{1/2} \cdot \exp\left(\frac{\lambda_{ADN}-\lambda}{4k_BT}\right)\right] \equiv \left(\frac{V_{ab}}{V_{ADN}}\right)^2 \cdot \gamma, \quad (2)$$

where k_{ADN} and V_{ADN} are, respectively, the hopping rate and charge-transfer integral for the un-substituted ADN. The left hand side of Eq. (2) is known from TOF measurements. The right hand of Eq. (2) can be divided into two parts: (i) the expression in the square bracket, which is denoted by γ, only depends on the reorganization energy λ, and (ii) $(V_{ab}/V_{ADN})^2$ which is controlled by the charge-transfer integral of ADN compounds. Both λ and V_{ab} may contribute to the reduction in the carrier mobilities after *t*-Bu substitution.

Table 1
Transport parameters of anthracene derivatives

Compounds	$\mu_{h,0}$ (10^{-8} cm^2/Vs)	Normalized $\mu_{h,0}$	λ_+ (eV)	γ	$\left(\frac{V_{ab}}{V_{ADN}}\right)^2$
ADN	3.53	1	0.33	1	1
TBADN	3.05	0.86	0.29	1.59	0.54
DTBADN	2.00	0.57	0.31	1.26	0.45
TTBADN	0.75	0.21	0.34	0.89	0.24

To delineate the contribution of λ and V_{ab}, we investigate the reorganization energies of the ADN compounds computationally. The ground state molecular structures were optimized at the unrestricted Hartree–Fock (HF) level with the 6-31G(d) basis set (UHF/6-31G(d)). Density functional theory (DFT) was applied to compute the Kohn–Sham molecular orbitals, employing the B3LYP/6-31G(d) density functional. Fig. 5 shows the frontier orbitals of ADN and TTBADN. The highest occupied molecular orbital (HOMO) and the lowest unoccupied molecular orbital (LUMO) in both ADN compounds are localized on the anthracene moiety and do not involve the naphthyl and *t*-Bu groups. So, the naphthyl and *t*-Bu groups effectively act as inert spacers for charge carriers transport. The computed hole reorganization energies, λ_+, are in the range 0.29–0.34 eV (Table 1, fourth column), and their values are shown in Fig. 4. In the case of un-substituted ADN, the hole reorganization energy $\lambda_{ADN} = 0.33$ eV. According to Eq. (2), if a particular ADN compound has $\lambda_+ < \lambda_{ADN}$, then the hole mobility tends to be enhanced because the factor $\gamma > 1$; conversely if the compound has $\lambda_+ > \lambda_{ADN}$, then the hole mobility tends to be reduced as $\gamma < 1$. Our computed results for TBADN and DTBADN have $\lambda_+ < \lambda_{ADN}$, yet the experimentally determined zero-field mobilities decrease relative to ADN. This analysis clear indicates that the reorganization energy alone is not adequate to account for the variation in the carrier mobilities in ADN compounds. Instead, the charge-transfer integral play a dominant role.

The last column of Table 1 indicated the ratio of the square of the charge-transfer integral $(V_{ab}/V_{ADN})^2$ evalu-

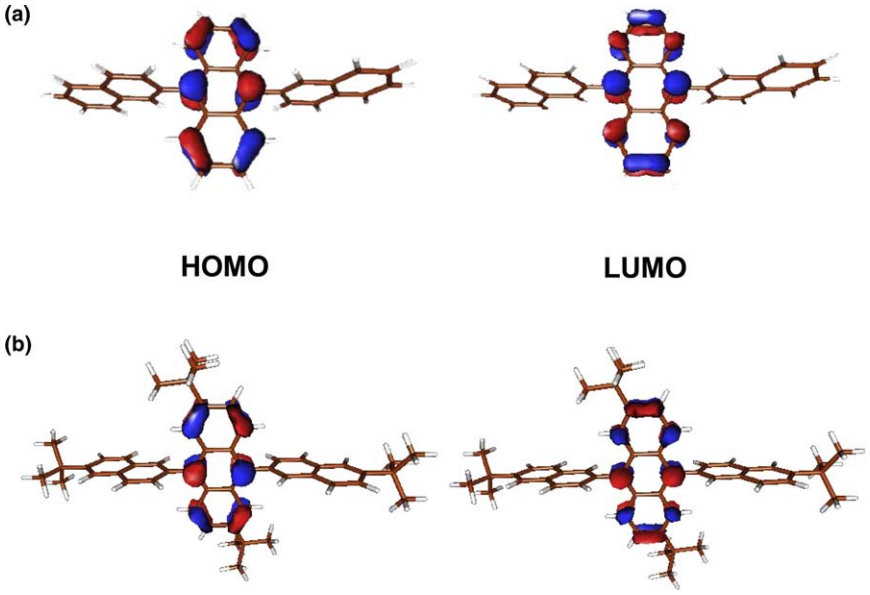

Fig. 5. The frontier orbitals of anthracene derivatives: (a) ADN; (b) TTBADN.

ated from experimental $\mu_{h,0}$ and computed γ. There is a gradual reduction of the charge-transfer integral in going from un-substituted ADN to the most heavily substituted TTBADN. As the charge-transfer integral is directly related to the electronic coupling between two adjacent molecules, the results can be understood in light of the reduced the electronic coupling, or an increase in the charge hopping distance, because of the presence of the electronically inert *t*-Bu group.

5. Conclusions

We show that *t*-Bu substitution is an effective means of tuning carrier mobilities in ADN compounds. By increasing the degree of *t*-Bu substitution, one can systematically suppress carrier mobility. The reduction in carrier mobility is mainly determined by the reduction in the charge-transfer integral. The present study can be potentially extended to other small π-conjugated molecules relevant to organic electronics, and offers a guideline for controlling the charge transporting properties of organic electronic materials.

Acknowledgements

Support of this research by the Research Grant Council under Grant #HKBU/2173/04E is gratefully acknowledged. This work is partially supported by the Incentive Fund of the Physics Department of The Chinese University of Hong Kong (CUHK), and was performed in part using the supercomputing system in CUHK's ITSC.

References

[1] See, e.g., G.R. Hutchison, M.A. Ratner, T.J. Marks, J. Am. Chem. Soc. 127 (2005) 2339.
[2] L.S. Hung, C.H. Chen, Mater. Sci. Eng. R 39 (2002) 143.
[3] R.Y. Wang, W.L. Jia, H. Aziz, G. Vamvounis, S. Wang, N.X. Hu, Z.D. Popovisć, J.A. Coggan, Adv. Funct. Mater. 15 (2005) 1483.
[4] C. Brabec, N. Sariciftci, J. Hummelen, Adv. Funct. Mater. 11 (2001) 15.
[5] H. Sirringhaus, Adv. Mater. 17 (2005) 2411.
[6] H.E. Katz, Z. Bao, J. Phys. Chem. B 104 (2000) 671.
[7] H. Bässler, Phys. Stat. Sol. B 175 (1993) 15.
[8] H.H. Fong, K.C. Lun, S.K. So, Chem. Phys. Lett. 353 (2002) 407.
[9] Rudolph A. Marcus, Rev. Mod. Phys. 65 (1993) 3.
[10] See, e.g., C. Risko, G.P. Kushto, Z.H. Kafafi, J.L. Bredas, J. Chem. Phys. 121 (2004) 9031.
[11] Bo Chao Lin, Cheu. P. Cheng, Zhi-Qiang You, Chao-Ping Hsu, J. Am. Chem. Soc. 127 (2005) 66.
[12] B.C. Lin, C.P. Cheng, Z.P.M. Lao, J. Phys. Chem. A 107 (2003) 5241.
[13] B. Balaganesan, W.J. Shen, C.H. Chen, Tetrahedron Lett. 44 (2003) 5747.
[14] J. Shi, C.W. Tang, Appl. Phys. Lett. 80 (2002) 3201.
[15] J.M. Shi, C.H. Chen, K.P. Klubek, US Patent 6,465,115 B2 (2002).
[16] H.H. Fong, S.K. So, J. Appl. Phys. 98 (2005) 023711.